Journal of Materials Chemistry B

Accepted Manuscript



This is an *Accepted Manuscript*, which has been through the Royal Society of Chemistry peer review process and has been accepted for publication.

Accepted Manuscripts are published online shortly after acceptance, before technical editing, formatting and proof reading. Using this free service, authors can make their results available to the community, in citable form, before we publish the edited article. We will replace this Accepted Manuscript with the edited and formatted Advance Article as soon as it is available.

You can find more information about *Accepted Manuscripts* in the **Information for Authors**.

Please note that technical editing may introduce minor changes to the text and/or graphics, which may alter content. The journal's standard <u>Terms & Conditions</u> and the <u>Ethical guidelines</u> still apply. In no event shall the Royal Society of Chemistry be held responsible for any errors or omissions in this *Accepted Manuscript* or any consequences arising from the use of any information it contains.



RSCPublishing

ARTICLE

A Photonic Glucose Biosensor for Chronic Wound Prognostics

Cite this: DOI: 10.1039/x0xx00000x

Fransiska S. H. Krismastuti, William L. A. Brooks, Martin J. Sweetman, Brent S. Sumerlin, $^{b^*}$ and Nicolas H. Voelcker $^{a^*}$

Received ooth January 2014, Accepted ooth January 2014

DOI: 10.1039/x0xx00000x

www.rsc.org/

The ability to monitor glucose levels in chronic wound fluid of diabetic patients is a promising theranostic approach in chronic wound healing. Phenylboronic acid polymers are glucose- and pH-responsive materials. In the presence of glucose, these polymers reversibly form cyclic boronate esters, changing the properties of the polymer and forming the basis of glucose sensing. In this report, poly(4-vinylphenylboronic acid) (PVPBA) was covalently grafted to the pores of porous silicon (pSi) films (pSi-PVPBA). Polymer switching in response to changing pH and glucose concentration was monitored by means of interferometric reflectance spectroscopy (IRS). We observed that a shift of the boronic acid equilibrium between the neutral and anionic form in the polymer translated into refractive index changes that could be detected as a variation of the effective optical thickness (EOT) of the pSi-PVPBA film. The pSi/polymer composite was further investigated as a platform for the detection of glucose. Using this sensing platform, we were able to detect glucose in a buffer solution as low as 0.15 mM and also in a wound fluid sample without encountering interferences.

Introduction

Diabetes mellitus is a chronic disease caused either by a lack of functional insulin produced by the pancreas or by insulin-resistance in the body. This results in an abnormal glucose concentration in the blood system. Recent data from World Health Organization (WHO) shows that approximately 150 million people worldwide suffer from diabetes mellitus, with this number predicted to double by 2025. Diabetes mellitus is associated with many other health problems and diseases. One of the common complications is the appearance of diabetic foot ulcers. The high concentration of glucose in the blood (hyperglycemia) causes the blood vessel constriction and the cell membrane to rigidify. This phenomenon hinders blood flow, leading to poor circulation of red blood cells to the feet, which causes foot ulceration.

The diabetic foot ulcer is characterized by an impaired or abnormal inflammatory cell function, a decreased secretion of cytokines or growth factors, a prolonged inflammatory phase⁶ and a delay in wound closure.⁷ These conditions make diabetic wounds often difficult to heal and lead to them becoming chronic. Therefore, an extra level of care and better wound management is required to treat diabetic wounds in order to prevent the chronicity of the wound, which may eventually lead to surgical intervention or amputations.

Good metabolic control and tight control of the glucose levels within the normal physiological range of 110 mg/dL \pm 25 mg/dL (6.1 mM \pm 1.4 mM) is an important therapeutic goal that helps minimize the incidence of diabetic foot ulcers. This underscores the importance of developing suitable diagnostic tools or point-of-care devices that can be easily used to measure the glucose level in physiological fluid, such as blood and wound fluid. Various detection techniques have been extensively studied. The first glucose

biosensor was based on an electrochemical detection mechanism and was proposed by Clark and Lyons from the Children's Hospital of Cincinnati in 1962.^{1, 8, 9} Electrochemical biosensors based on enzymatic amperometric detection have seen tremendous success and several generations are on the market.⁸ Most commercially available sensors are test-strip based with the strip containing enzymes, coenzymes, mediators and indicators which convert the glucose level in the blood into a specific signal, readable by a handheld device.¹⁰ The application of this glucose sensor is mainly for human blood samples.

Until now, a correlation between the glucose level in the blood serum of diabetic people and diabetic wound fluid during the wound healing process has not been established. One report from Velander et al. studied the effect of the high concentration of glucose (hyperglycemia) in diabetic wound healing, using diabetic pigs as a model. The authors observed that in wounded diabetic pigs the initial glucose concentration in the wound fluid was at the same level as in the blood serum until 5 days post wound inducement, after which the concentration of glucose in the wound fluid decreased to undetectable levels, with the wound being healed on day 9. In contrast, in the wound fluid of non-diabetic pigs, the concentration of glucose was undetectable from day 1.7 This finding indicates that the level of glucose in wound fluid is closely associated with the healing status of the diabetic wounds and the level of glucose in the blood.⁷ This also suggests that monitoring the glucose level in diabetic wound fluid may be an important prognostic indicator of the healing status of diabetic wounds and that glucose measurement in wound fluid may assist diabetic wounds management.

In addition to the electrochemical detection technique, there is an alternative advanced approach for glucose detection utilizing a stimuli-responsive material, such as polymer. Stimuli-responsive polymers are polymers that response to physical or chemical stimuli by changing their structure, individual chain dimensions, solubility

or the degree of intermolecular association.¹¹ Recent investigation into these 'smart' polymers have drawn attention due to their wide promising applications, particularly in biomedical applications, such as drug delivery, sensing and diagnostics.¹¹⁻¹⁴ One promising class of stimuli-responsive materials is polymers containing boronic acid functionalities.

ARTICLE

Boronic acid-containing polymers are glucose and pH stimuliresponsive. 11, 12, 15-17 In aqueous media, boronic acid exists in equilibrium between forms that are neutral/trigonal and anionic/tetrahedral. The direction of the equilibrium can easily be adjusted depending on the pK_a of boronic acid, solution pH and addition of diols. ¹⁸ At pH values below the pK_a , the boronic acid is neutral and hydrophobic. Phenylboronic acid polymers are therefore typically insoluble in aqueous solution at low pH. In contrast at high pH (pH > p K_a), the boronic acid is the anionic/hydrophilic form and soluble in an aqueous solution. The addition of 1,2- or 1,3-diols, such as those in glucose, shifts the ionization equilibrium to the anionic and hydrophilic boronate. This behavior arises because while cyclic esters formed between diols and neutral boronic acid are hydrolytically labile, esters formed with the tetrahedral anionic boronate species are generally stable. 17-20 This behavior of the boronic acid polymer and its derivatives can therefore be exploited for pH and glucose sensing. Further expanding the scope of these systems is achieved through modification with other responsive polymers forming block copolymers containing boronic acid moieties that response to other stimuli in addition to pH and glucose.17

The properties of boronic acid responsive polymers, including the reversible binding and detection of sugars (e.g., glucose and fructose) in an aqueous environment, have been thoroughly studied and reported. ^{11, 17, 18, 20, 21} Along with solution detection systems, boronic acid polymers have also been immobilized on certain materials such as gold²² or carbon nanotubes¹⁹, coated onto platinum electrodes²³ and combined with hydrogels^{24, 25} or other polymers to form a photonic polymer. ²⁶ The versatility of these materials provides opportunities for further application as point-of-care devices or implantable real-time glucose monitoring systems.

pSi is a nanostructure material with a large surface area up to 800 m²/g that has unique optical and morphological properties. ^{27, 28} This material has been extensively studied for biosensing applications. ^{27, 29-32} A pSi thin film is fabricated from a bulk silicon wafer by a simple electrochemical anodization process. ^{27, 33-36} The anodization parameters can be tuned to achieve the desired morphological structures, including intricate multilayers. ²⁷ Therefore, for sensing applications, the pSi structure can be designed and optimized to suit a specific target analyte allowing the ingress of biomolecules throughout the porous matrix. In addition, the biocompatibility and biodegradability of pSi facilitate implantable sensor applications. ^{33, 37} All of the above-mentioned advantages suggest that pSi is ideally suited as a perfect matrix to immobilize the responsive boronic acid polymer to develop an optical glucose sensing platform.

The optical properties of the pSi film can be easily monitored by interformetric reflectance spectroscopy (IRS). Incident white light is reflected from two interfaces of a single layer pSi film (air/pSi and pSi/bulk silicon), with the reflected light generating a fringe pattern or so called Fabry-Pérot interference pattern. The position of the fringe maxima is determined by equation 1. ^{27, 31, 34-36}

$$m\lambda = 2nL \tag{1}$$

In equation 1, m is the fringe order, λ is the wavelength of incident light for maximum constructive interferences, n is the refractive index of the porous film, L is the film thickness and the factor of 2 is derived from the factor of 90 ° backscatter configuration of the light source and detector. ^{27, 31, 34, 35} The effective optical thickness (EOT),

the product of refractive index and the thickness, is highly sensitive to changes within the porous layer. The EOT therefore can be used to monitor changes in binding or unbinding of molecules and also changes in the properties of the molecules embedded within the porous layer of pSi. 34-36, 38 This principle is widely used in optical biosensing based on pSi. 27, 31, 39

More complex structures, such as a pSi rugate filters (pSiRF) are also used in optical biosensing. The pSiRF is a photonic structure, fabricated by sinusoidally alternating between low and high current density which leads to periodic low and high porosity layers. ⁴⁰ The resulting photonic stop band leads to a reflectivity peak that is sensitive to changes in refractive index. ^{41, 42} A small change in the refractive index within the pores induces a large shift in the photonic peak, leading to a sensitive optical transducing mechanism for biosensing applications. ⁴³

The infiltration of polymers into pSi for sensing purposes has been pursued previously. ^{35, 36, 44-46} The polymers were either spin-coated ^{44, 45}, grafted from ^{35, 36} or grafted to ⁴⁷ the pSi. Alternatively, hydrogels were formed inside of the porous layer. ⁴⁸ In some cases, purpose of polymer deposition was to increase the stability and prevent the degradation of pSi surface in slightly basic medium during sensing. ^{44, 45} In other cases, responsive polymers were employed to detect changes in pH⁴⁷ or temperature. ^{35, 36, 48}

In this study, we grafted thiol-terminated poly(4-vinylphenylboronic acid) (PVPBA-SH) onto porous silicon reflector films. The response of the polymer to changing pH and the addition of glucose at physiological pH was optically monitored by measuring the EOT changes by means of IRS and changes in the reflectivity peak of a pSiRF, respectively. The sensitivity of the resulting glucose sensors was optimized by tuning the pore parameters. The optimum conditions were then tested over a range of glucose concentrations in a buffer solution. Finally a real application of this sensing platform, to selectively and sensitively detect the glucose levels in a human wound fluid sample, was also demonstrated.

Experimental section

Materials

2-Dodecylsulfanylthiocarbonylsulfanyl-2-methylpropionic acid (DMP) was prepared as previously reported.⁴⁹ N,Ndimethylacrylamide (DMA, TCI, 98%) was passed through a small column of basic alumina prior to polymerization. 2,2'azobisisobutyronitrile (AIBN, Sigma, 98%) was recrystallized from ethanol. Dichloromethane (DCM, Macron, ACS grade) was dried over molecular sieves before use. Pinacol (Acros Organics, 99%), 4-vinylphenylboronic acid (CombiBlocks, 98%), N,N-dimethylformamide (DMF, Acros Organics, >99%), hexane (BDH, 98.5 %) N,N-dimethylacetamide (DMAC, Acros 99%), benzene (Sigma Aldrich, 99%), lithium chloride (Acros, 99%), hydrazine monohydrate (Alfa Aesar, dimethylsulfoxide-d6 (DMSO-d₆, Cambridge Isotope, 99.9% D), chloroform-d (CDCl₃, Cambridge Isotope, 99.8% D), methanol-d₄ (MeOD, Cambridge Isotope, 99.8% D), and polystyrene supported boronic acid resin (Lancaster) were used as received. Dialysis was conducted with Spectrum Labs regenerated-cellulose membranes with 3,000 Da molecular weight cut-off (MWCO).

Synthesis of 4-vinylphenylboronic acid pinacol ester

4-vinylphenylboronic acid pinacol ester (VPBAE) was prepared as previously reported.⁵⁰ Activated molecular sieves (1 g) were added

to a 250 mL round bottom flask. DCM (100 mL) was added, and the mixture was rapidly stirred while VPBAE (5.0 g, 33.8 mmol) and pinacol (4.2 g, 35.5 mmol) were added. The mixture was stirred for 18 h, and the molecular sieves were removed by filtration and washing with DCM (100 mL). The filtrate was concentrated under vacuum to give a colorless oil.

RAFT polymerization of VPBAE

VPBAE (4.05 g, 17.6 mmol), DMP (42.7 mg, 0.118 mmol), AIBN (5.8 mg, 0.035 mmol), and trioxane (79.2 mg) were dissolved in benzene (8.0 mL) in a sealed 20-mL vial. The vial was purged with nitrogen for 30 min and then placed in a preheated reaction block at 70 °C. Samples were removed periodically by syringe to determine monomer conversion by ¹H NMR spectroscopy. CDCl₃ was used as the solvent for NMR spectroscopy. The resulting polymer was purified by precipitation three times into cold hexane. ($M_{n,theo}$ = 19,800 g/mol, $M_{n,GPC}$ = 22,500 g/mol, M_{w}/M_{n} = 1.02).

Deprotection of VPBAE

Poly(VPBAE) (PVPBAE) (0.475 g, 0.0279 mmol) and polystyrene-supported boronic acid resin (5.31 g, 14.8 mmol, boronic acid loading 2.6–3.0 mmol/g) were stirred and refluxed for 24 h in a 2 vol % solution of trifluoroacetic acid in acetonitrile (60.0 mL) in a 100-mL round bottom flask. The solvent was removed under reduced pressure, and DMF/deionized water (95/5) (60 mL) was added to the product. The solution was filtered to recover the polystyrene-supported boronic acid resin, and the solvent was removed under reduced pressure. The remaining solid was dissolved in 2 wt/vol % aqueous NaOH (10 mL) and dialyzed against 2 wt/vol % aqueous NaOH, followed by dialysis against deionized water. The resulting solution was lyophilized to yield the dry poly(4-vinylphenylboronic acid) (PVPBA) polymer (0.29 g, $M_{\rm n,deprotected} \sim 14,500 \ {\rm g/mol})$.

Synthesis of PVPBA-SH

PVPBA (0.25 g, 0.023 mmol) was dissolved in a 95:5 vol/vol solution of DMF/water (10 mL) and purged with nitrogen gas. To this solution was added hydrazine monohydrate (25 μ L). The solution was allowed to stir overnight before being dialyzed against 2 wt/vol % aqueous NaOH, followed by dialysis against deionized water. The resulting solution was lyophilized to yield a white powder (0.23 g).

RAFT polymerization of DMA

DMA (2.0 g, 20.2 mmol), DMP (18.4 mg, 0.0504 mmol), AIBN (0.80 mg, 4.88 x 10^{-3} mmol), and trioxane (90.8 mg) were dissolved in dioxane (10.0 mL) in a sealed 20-mL vial. The vial was purged with nitrogen for 30 min and placed in a preheated reaction block at 60 °C. Samples were removed periodically by syringe to determine monomer conversion by ¹H NMR spectroscopy. CDCl₃ was used as the solvent for NMR spectroscopy. The resulting polymer was purified by precipitation three times into cold hexane. ($M_{\rm n,theo} = 26,000$ g/mol $M_{\rm n} = 25,400$ g/mol, $M_{\rm w}/M_{\rm n} = 1.01$).

Synthesis of PDMA-SH

PDMA (0.50 g, 0.0192 mmol) was dissolved in THF and purged with nitrogen. To this solution was added hydrazine monohydrate (10 μ L). The solution was allowed to stir overnight before being

dialyzed against deionized water. The resulting solution was lyophilized to yield a white powder (0.48 g).

Polymer characterization

Size exclusion chromatography (SEC) for PVPBAE was conducted in DMAC (with 0.05 M LiCl) at 50 °C with a flow rate of 1.0 mL/min (Pump: Agilent 1260 Infinity Isocratic Pump G1310B, Columns: Guard + two ViscoGel I-series G3078 mixed bed columns, molecular weight range $0-20\times10^3$ and $0-100\times10^4$ g mol⁻¹). Detection consisted of a Wyatt Optilab T-rEX refractive index detector operating at 658 nm and a Wyatt miniDAWN TREOS laser light scattering detector (operating at 50 mW, 658 nm with detection angles of 49°, 90°, and 131°). Molecular weights were determined using measured dn/dc values for PDMA and PVPBAE of 0.0699 and 0.0725 mL/g, respectively.

Fabrication and characterization of pSi samples

All pSi samples were prepared from (100)-oriented, highly-boron doped p-type Si wafer with 0.00055 – 0.001 Ω cm resistivity and 475 – 525 μ m thickness (Siltronix). The pSi samples were fabricated by an electrochemical etching process in a Teflon-based cell using aluminium tape as the anode placed at the backside of Si wafer and a platinum mesh as the cathode placed in the middle of the etching cell, at a certain height from the Si wafer. The electrochemical etching solution contained a 1:1 volume ratio of aqueous hydrofluoric acid (48%, Scharlau) / high purity ethanol (Chem Supply).

The Si wafer was etched at a current density of 28.3 mA/cm² for 30 s and then exposed to 0.1 M sodium hydroxide solution for 2 min to dissolve the initial porous layer. This step was performed in order to remove the parasitic layer. This step was performed in order to remove the parasitic layer. Following this step, the surface was washed three times with MilliQ water and ethanol and dried under a stream of nitrogen gas. The pre-treated surface was then etched at different current densities and times as shown in Table 1. The pSiRF was fabricated by sinusoidally varying the current density between 5.7 mA/cm² and 28.3 mA/cm² for 15 periods with an etching time of 3.2 s for each period. pSi samples were characterized by scanning electron microscopy (SEM) using a Quanta 450 field emission gun (FEG) Environmental SEM fitted with a solid-state detector (SSD) at an accelerating voltage of 30 kV.

Surface functionalization

The freshly etched pSi samples were thermally oxidized at 600 °C for 30 min, followed by ozone oxidation for 1 h. The thermal oxidation was performed in a Labec tube furnace (Laboratory equipment Pty. Ltd), while the ozone oxidation was performed using an ozone generator (Fischer, Ozone Generator 500) at a flow rate of 100 L/h producing 3.25 g/h of ozone.

Silanization chemistry was then carried out on the oxidised pSi surface using 50 mM (3-aminopropyl)triethoxysilane (APTES, Sigma-Aldrich) in anhydrous toluene (Sigma-Aldrich) while shaking the sample for 10 min at room temperature. Afterwards, the samples were removed from the silane solution, washed with anhydrous toluene three times and dried under a stream of nitrogen gas.

The silanized pSi samples were then reacted with freshly prepared 25 mM succinimidyl 4-(p-maleimidophenyl)butyrate (SMPB, Pierce) in dimethylsulfoxide (DMSO, Chem Supply) for 30 min at room temperature. The surface was then washed using DMSO and ethanol three times and dried under a stream of nitrogen gas.

Finally, the PVPBA-SH (p $K_a = 9$) was immobilized on the pSi modified surface. 0.9 mM of PVPBA-SH in 1:1 volume ratio of DMF/MilliQ water was reacted with the pSi modified surface for 17

h at room temperature. As a control, a separate SMPB-modified pSi surface was reacted with 0.9 mM of thiol modified PDMA-SH in MilliQ water for 17 h at room temperature. The pSi/polymer composite surface was rinsed with water, 2:1 water/ethanol, 1:2 water/ethanol, and ethanol and then dried under a stream of nitrogen

Diffuse reflectance infrared Fourier transform (DRIFT) spectroscopy

IR spectra were obtained using a Thermo Nicolet Avatar 370MCT (Thermo Electron Corporation) instrument with a smart diffuse reflectance accessory and OMNIC version 7.3 software to record and analyze the spectra. All spectra were recorded over the range of 400 – 4000 cm⁻¹, at a resolution of 4 cm⁻¹ and averaging 64 scans. The background spectra were taken using a suitable clean unetched Si wafer, and sample spectra were taken after every surface functionalization step.

Interferometric reflectance spectroscopy (IRS)

The reflectance spectra of the pSi samples were acquired using an Ocean Optics spectrometer. White light from a tungsten lamp was fed through one end of a bifurcated fiber-optic cable and focused through a lens onto the surface of pSi sample clamped in a custom-made aqueous flow cell. The reflected light was collected through the same optics connected to a charge coupled device (CCD) detector (Ocean Optics S2000). The data were collected using a custom LabView program, and the EOT was obtained by performing a fast Fourier transformation of the recorded interferometric reflectance spectra (Wavemetrics Inc. Igor program).

Glucose sensing experiments

ARTICLE

An aqueous glucose stock solution (0.25 M) was prepared from 99.5% of D-(+)-glucose (Sigma) in a Hepes (Sigma-Aldrich) buffer solution at pH 7.4 (100 mM Hepes, 115 mM NaCl). The glucose stock solution was prepared at least 24 h prior to use in order to establish the mutarotation equilibrium.²⁵

The biosensing experiments were carried out in a custom-made aqueous flow cell at room temperature. The fully functionalized pSi with PVPBA-SH polymer (pSi-PVPBA) as a sample surface was immersed in the Hepes buffer solution at pH 7.4 with a flow rate of 0.3 mL/min. EOT readings were recorded every min for a period of 10 min. 10 mM of glucose at pH 7.4 was then flowed through the cell for 10 min, and the EOT readings were recorded. This switching cycle was repeated 5 times with the EOT being consistently measured for every min. The same buffer/glucose biosensing experiment was also performed using the pSi surface modified using PDMA-SH polymer (pSi-PDMA) as a control.

Wound fluid experiments

Wound fluid was collected from patients with chronic venous leg ulcers at the Queen Elizabeth Hospital (South Australia, Australia). The study protocol conformed to the ethical guidelines of the 1975 Declaration of Helsinki and was approved by the Health Service Human Research Ethics Committee and Central Northern Adelaide Health Service Ethics of Human Research Committee. The biosensing experiments for wound fluid samples were conducted in a similar way as glucose sensing in buffer solution as previously described. The pSi-PVPBA samples were immersed in the Hepes buffer solution at pH 7.4 and the EOT readings were recorded every min for 10 min. Following this, a 10-fold dilution of wound fluid (in MilliQ $\rm H_2O$) was then introduced to the flow cell using a 500 µL

syringe, and the EOT readings were recorded for 10 min. This switching cycle was also repeated 5 times. The same protocol was also conducted for a 10-fold dilution of wound fluid spiked with 10 mM of glucose, a 10-fold dilution of wound fluid sample at pH 7.5 (the pH was adjusted to 7.5 using Hepes buffer solution) and a 10-fold dilution of wound fluid at pH 7.5 spiked with 10 mM of glucose.

Results and discussion

Preparation of the optical transducer

The single layer pSi film was prepared from p-type silicon wafer by electrochemical etching with an etching solution containing HF and ethanol (1:1 volume ratio). Eight different conditions for fabricating the pSi films, as listed in Table 1, were tested to determine the optimum pore size and thickness for sensing (explained in the next section). The etching parameters, such as current density and etching time were adjusted to obtain different pore sizes and film thickness values. Higher current density applied during etching resulted in larger pore diameters, and for constant current density, longer etching times resulted in thicker porous layers. These results were confirmed by SEM.

Table 1. Etching conditions used to fabricate the single layer pSi samples in this study and the resulting film parameters.

	G .		ъ	D	
Surface No.	Current density (mA/cm ²)	Ething time (s)	Pore size (nm)	Pore thickness (nm)	Porosity (%)
				.=	
1	2.8	1626	12-21	1741.5	46.2
2	5.7	810	18-29	2162.8	50.6
3	28.3	150	25-40	2157.9	58.7
4	56.6	80	33-53	2227.4	67.0
5	5.7	375	18-29	1001.3	50.6
6	5.7	560	18-29	1495.2	50.6
7	5.7	1111	18-29	2966.4	50.6
8	5.7	1625	18-29	4339.0	50.6

IRS was used to collect the fringe patterns of the single layer pSi for each different etching condition. The fringe pattern obtained from the light reflected from the top and bottom interface of the single layer pSi was then normalized to 100% reflectance from flat silicon as a background in order to obtain the absolute reflectance spectrum of the single layer pSi. A best fit calculation of the reflectance spectrum of the single layer pSi and the theoretical spectrum using the transfer matrix method was used to determine the porosity of pSi³⁵ shown in Table 1.

Functionalization and characterization of pSi surfaces

The freshly etched pSi surface was chemically modified prior to attaching the PVPBA-SH polymer. The surface was firstly thermally oxidized at 600 °C for 30 min (Figure 1, (a)) to stabilize the pSi. Oxygen present during the thermal oxidation attacked the back-

bonds of the hydrogen terminated pSi surface, replaced the hydrogen atoms and formed oxygen bridges between the surface Si atoms and the second atomic Si layer.⁵⁴ This helped to protect the pSi surface and reduces the rate of hydrolysis in an aqueous environment, which is unacceptable for sensing applications. The thermal oxidation was then followed by ozone oxidation for 1 h (Figure 1, (b)), which generated silanol (-SiOH) species on the pSi surface that were further reacted with the ethoxy groups of APTES during the silanization process (Figure 1, (c)). The introduced amine groups were then reacted with SMPB as a cross-linker, through amide bond formation (Figure 1, (d)). SMPB is a maleimide functionalized cross-linker, useful for coupling with reactive thiol groups. This linker allowed PVPBA-SH to be covalently attached onto the pSi surface. Throughout the rest of this paper, the fully functionalized pSi surface is referred to as pSi-PVPBA (Figure 1, (e)). The surface reaction steps are shown in Figure 1.

Figure 1. Functionalization steps for the fabrication of pSi-PVPBA films; (a) thermal oxidation, (b) ozone oxidation, (c) APTES silanization, (d) SMPB cross-linker attachment and (e) PVPBA grafting.

DRIFT spectroscopy was used to characterize the pSi surface after each surface modification reaction step (Figure 2). The formation of silicon back-bonds during the thermal oxidation process (Spectrum (a)) of freshly etched pSi was observed as a broad peak at 1100 cm⁻¹ corresponding to Si-O-Si stretching modes.⁵⁵ The absence of Si-H_x stretching at 2100 cm⁻¹ indicates that the surface was completely oxidized.⁵⁵ The thermally oxidized pSi surface was then treated using ozone (Spectrum (b)) for 1 h to produce Si-OH species on the pSi surface, which enables effective silanization.⁵⁶ This was evidenced by the increase in intensity of a peak at 3740 cm⁻¹. ^{56, 57} A two-step oxidation procedure was required to generate a stable

surface that is less susceptible to hydrolytic attack and also to provide enough silanol groups to facilitate the silanization process.

The next step was the silanization of the oxidized pSi surface using APTES. The ethoxy groups of APTES react with free silanol groups on the oxidized pSi surface by S_N2 exchange. The IR spectrum after APTES modification (Spectrum (c)) shows bands at 1570 cm⁻¹ and 2920 cm⁻¹ corresponding to NH_2 scissor vibration of the amine terminus and the methylene valence vibrations of the APTES, respectively, confirming the attachment of the APTES on the pSi surface. In addition, small peaks were observed at 1635 cm⁻¹ and 1484 cm⁻¹ which were attributed to the asymmetric and symmetric $-NH_3^+$ deformation mode, respectively. At the same time, the silanol peak at 3740 cm⁻¹ disappeared.

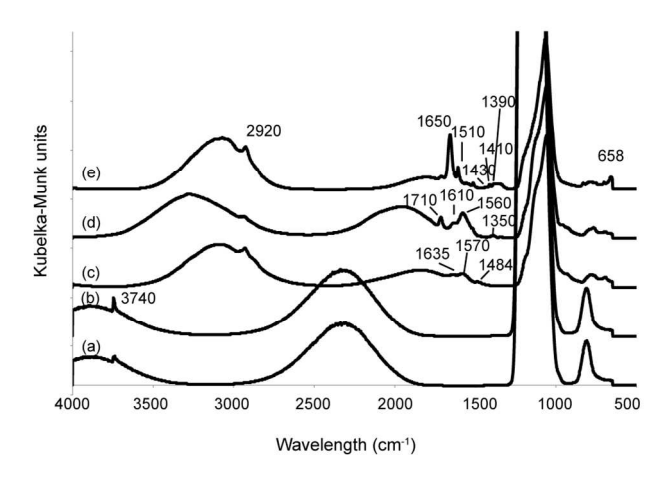


Figure 2. Infrared spectra for each surface modification reaction step: (a) thermal oxidation, (b) ozone treatment, (c) APTES silanization, (d) maleimide reaction and (e) PVPBA-SH polymer attachment.

The amine terminated pSi surface was then reacted with SMPB in order to facilitate polymer attachment on the pSi surface. After reaction with SMPB (Spectrum (d)), the bands characteristic with the –C=O asymmetric stretching mode and C–N–C symmetric stretching band of maleimide appeared at 1710 cm⁻¹ and 1350 cm⁻¹, respectively. ⁶⁰ In addition, the band attributed to amide I and amide II at 1610 cm⁻¹ and 1560 cm⁻¹ respectively, gave an indication that the attachment of maleimide functional crosslinker on the pSi surface was through formation of an amide bond.

PVPBA-SH was then reacted on the maleimide terminated pSi surface (Spectrum (e)). The conspicuous peak at 1650 cm⁻¹ was attributed to the C=C aromatic of the phenyl group from the phenylboronic acid containing polymer. ^{61, 62} The peak at 1390 cm⁻¹ corresponds to the vibration band of B=O of the phenylboronic acid polymer. ^{61, 62} The weak bands at 1510 cm⁻¹, 1430 cm⁻¹ and 1410 cm⁻¹ were assigned to the C=C vibration of the phenylboronic acid. ⁶² In addition, the weak band at 658 cm⁻¹ attributed to the C=S stretching between the sulfur from the thiol of the polymer and carbon from the maleimide group on the modified pSi surface. The presence of all these peaks illustrates the successful grafting of the PVPBA on the pSi surface.

The pSi-PVPBA surface as a pH sensor

The responsiveness of the boronic acid-containing polymer in solution has been extensively studied by Sumerlin *et al.*, ^{11, 17, 18, 20, 21, ^{50, 63} along with various other research groups. ⁶⁴⁻⁶⁶ The boronic acid groups of the polymer in solution are either in a neutral trigonal form}

or the anionic tetrahedral form, with the relative concentration of each affecting the solubility of the polymer. Raising the pH of the solution and the addition of glucose or other diols at a fixed pH 7.4 have been recognized as factors that shift the equilibrium of the polymer toward the water-soluble state.

ARTICLE

Here, the behavior of the pSi-PVPBA, with $pK_a = 9$, was investigated by monitoring the EOT changes of the pSi-PVPBA by means of IRS. The experiments were conducted in a custom-made flow cell. A Hepes buffer solution at different pH (between pH 7 and pH 11) was flowed across the pSi-PVPBA surface that was being monitored by IRS. The EOT was then measured and recorded over time. As a control experiment, the maleimide-terminated pSi surface was reacted with PDMA-SH, a polymer that is not responsive to pH or glucose. The surface modification reaction was similar to the attachment of PVPBA-SH. To confirm the attachment of the PDMA, the surface was also characterized using DRIFT (Supporting information, Figure S2). The sensing experiments for pSi-PDMA surface were done in a similar way to the pSi-PVPBA surface. A typical experiment is displayed in Figure 3.

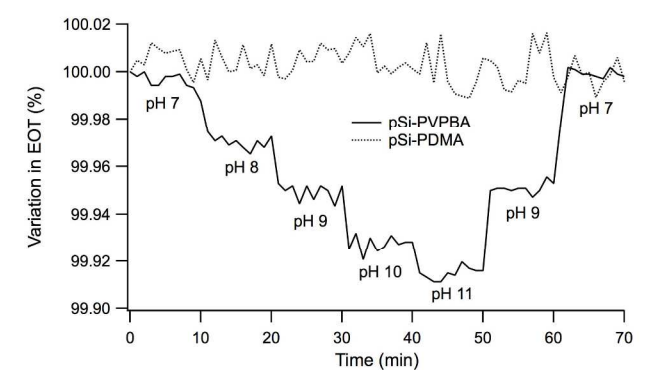


Figure 3. The variation in EOT of the pSi-PVPBA (solid line) and pSi-PDMA (dotted line) in Hepes buffer solution at different pH values.

In Figure 3 (solid line), a decrease in EOT (0.025%) was observed upon changing the buffer solution from pH 7 (0 – 10 min) to pH 8 (11 – 20 min). The EOT of the pSi-PVPBA experienced a gradual decrease of 0.024%, 0.021% and 0.017% when the pH of the buffer solution changed from pH 8 to pH 9 (21 – 30 min), pH 9 to pH 10 (31 – 40 min) and pH 10 to pH 11 (41 – 50 min), respectively. The reverse effect was observed upon changing the buffer solution back to pH 9 (min 51-60) and finally pH 7 (min 61-70), with EOT increases of 0.035% and 0.045% being measured, and the original EOT value was restored. The control experiment using pSi-PDMA surface, as seen in Figure 3 (dotted line), did not show any response when exposed to buffer solution at different pH, confirming that the change in the EOT in pSi-PVPBA surface was due to the polymer responding to the pH change.

The decrease in EOT observed in the pSi-PVPBA surface with increasing pH of the solution from pH 7 to pH 11 was attributed to the decrease in the refractive index of the pSi/polymer composite. It is assumed that initially, at neutral pH, the net refractive index is dominated by the refractive index of the polymer (\sim 1.49 - 1.5) and at higher pH, by the refractive index of the buffer solution (\sim 1.3). This is consistent with the boronic acid of the PVPBA being in the neutral form at pH 7, where there is no charge interaction between phenylboronic acid polymers. In addition, the phenyl group of the phenylboronic acid is hydrophobic, which prevents hydrogen bonding between water and hydroxyl groups of the boronic acid. Those conditions therefore cause the polymer to collapse and the

pSi-PVPBA surface to become hydrophobic. The hydrophobicity of the pSi-PVPBA surface limits the infiltration of the buffer solution throughout the porous layer, thus the net refractive index is dominated by the refractive index of the polymer filling the pores.

Increasing the pH of solution shifts the ionization equilibrium of the phenylboronic acid to the anionic form. The higher the pH, the more phenylboronic acid is in the anionic form. The negative charge of the polymer causes the grafted polymer chains to repel each other, thus the polymer is expanded and allows the infiltration of the buffer solution. In addition, the negative charged of the phenylboronic acid polymer also enables the formation of hydrogen bonding with water. The surface therefore becomes more hydrophilic and the net refractive index approaches that of the refractive index of the solution. This effect is reversible, as the experiment in Figure 3 shows.

The results confirm that the configuration of the polymer and the state of equilibrium of the boronic acid groups affect the optical properties of the pSi-PVPBA film. The behavior of the phenylboronic acid is in agreement with the behavior of the polymer in solution. This emphasizes that the phenylboronic acid polymer is able to retain its reversible switching properties in response to pH changes even after being grafted to a porous support such as pSi.

The pSi-PVPBA film as a glucose sensor

A further optical study on the responsiveness of pSi-PVPBA was carried out to investigate the response of the immobilized polymer to a glucose solution at physiological pH (pH 7.4). In solution, boronic acid interacts with glucose molecules to form cyclic boronate esters. ^{18, 20, 21, 26, 67} On the pSi surface, the behavior of the grafted polymer was again studied using IRS by monitoring the optical response over time, as shown in Figure 4 (solid line).

The sensorgram seen in Figure 4 shows a reversible and fast (within 1 min) decrease in EOT when pSi-PVPBA was exposed to buffer solution containing 10 mM glucose (indicated as 'glucose' in Figure 4). The EOT returned to the original level when the surface was exposed to buffer solution at pH 7.4 containing no glucose (indicated as 'buffer' in Figure 4). The decrease of net refractive index of the porous layer in the presence of 10 mM glucose is not due to a change of bulk refractive index in the buffer. Instead, the reversible switching corresponds to the formation and disassembly of the negatively charged and hydrophilic cyclic boronate ester between the boronic acid groups of PVPBA and glucose. 17, 18, 20, 21, 67 The formation of the anionic ester leads into a conformational change in the polymer due to polyanion formation and infiltration of buffer solution into the pores, reducing the refractive index. Removing the glucose from the buffer, leads to disassembly of the cyclic ester, restoring the neutral and hydrophobic form of the phenylboronic acid.

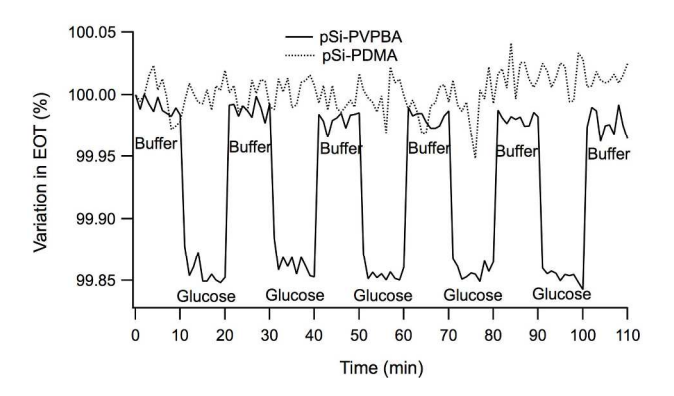


Figure 4. Variation in EOT of the pSi-PVPBA (full line) and pSi-

PDMA (dotted line) when exposed to buffer solution at pH 7.4 and in buffer solution at pH 7.4 containing 10 mM glucose.

This optical behaviour of the grafted polymer in the glucose solution is similar to what was observed when the pSi-PVPBA was exposed to buffer solution (Figure 3) where the pH > pKa of PVPBA $(pK_a = 9)$. It is also consistent with previous reports of the polymer's response to glucose in solution. 11, 17, 18, 20, 21, 50, 63-65 The addition of glucose at physiological pH on the pSi-PVPBA has a similar effect to the high pH (above the pK_a of the polymer), leading to a dramatic change in the ionization equilibrium of phenylboronic acid polymer, which is very useful if it is applied as a glucose biosensor at physiological pH. Our results so far indicate that immobilization of the phenylboronic acid polymer to a pSi surface retains the responsiveness of the polymer.

The control experiment using pSi-PDMA surface did not show any response when exposed to 10 mM glucose (dotted line, Figure 4). The result from the control sample confirms that the change in EOT observed for the pSi-PVPBA sample was due to the reversible assembly or disassembly of the boronate ester and not simply from the presence of glucose in solution.

Optimization of the architecture of single layer pSi for glucose sensing

The previous two experiments demonstrate the viability of pH and glucose sensing using the pSi-PVPBA composite. The next step was to optimize the morphological structure of the single layer pSi, including pore size and porous layer thickness in order to achieve high performance glucose sensing. Eight different pSi-PVPBA surfaces (each with different etching conditions) were prepared and tested (as listed in Table 1).

The responsiveness of the boronic acid polymer grafted to the pSi surface was again measured by monitoring the EOT when the surface was exposed to a buffer solution at pH 7.4 for 10 min followed by 10 mM of glucose solution at pH 7.4 for 10 min. The polymer switching was observed for 5 cycles forming a typical sensorgram similar to the sensorgram displayed in Figure 4. The percentage of the EOT decrease (ΔEOT) for each cycle was determined, and an average was calculated from 5 cycles. The percentages of ΔEOT for eight different pSi-PVPBA samples are shown in Figure 5.

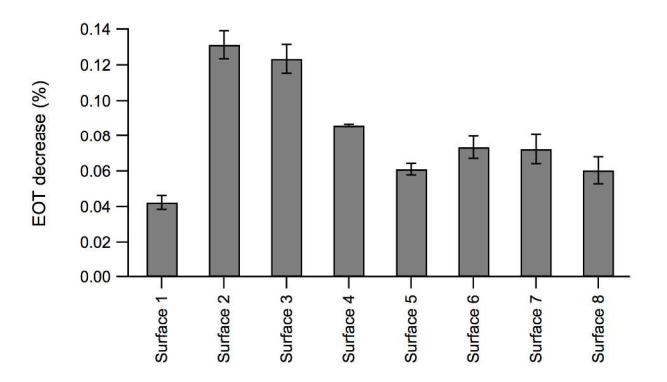


Figure 5. The percentage EOT decrease of the pSi-PVPBA measured by means of IRS for eight different conditions of single layer pSi (as listed in Table 1), as a response to 10 mM glucose at pH 7.4. The reported error has been calculated from the average of five cycles from three separate experiments.

pSi-PVPBA surfaces 1 to 4 (the number refers to the etching condition in Table 1) corresponds to different pore sizes ranging from smaller to bigger pores, with approximately the same film thickness (~ 2 µm). From Figure 5, it can be seen that the lowest response or the smallest ΔEOT (0.04%) was given by the pSi-PVPBA surface prepared from the pSi etched at the lowest current density (2.8 mA/cm²). These conditions produced the smallest pore size ranging from 12 nm to 21 nm (surface 1). For the higher current density, 5.7 mA/cm² (surface 2), larger pores of 18 – 29 nm were produced. The pSi-PVPBA surface prepared using these conditions producing the greatest change in EOT (Δ EOT = 0.13%), out of all the surfaces tested. Further increases in current density (surface 3 and 4) increased the diameter of the pores but led to reduced EOT sensitivity (0.12% for surface 3 and 0.09% for surface 4).

Considering these results, it was clear that pore size did affect the switching of the immobilized PVPBA, with the optimum conditions being achieved with surface 2 that had a pore size of 18 – 29 nm. The small pore diameter (surface 1) may restrict the PVPBA from expanding when binding to the glucose molecules. As the pore size increased (surface 2), more space was available for the polymer to expand after binding to the glucose molecules. However, a further increase in pore size, as for surface 3 and 4, saw the \Box EOT decrease. The pore diameter for surface 3 and 4 was assumed to be too large for to be fully filled by the grafted polymer, therefore leading to a mixture of buffer and polymer in the pores even when the boronic acid is in the neutral state. Therefore, polymer switching in these large pores has a smaller impact on the net refractive index than for the surface with optimal pore size range.

The current density for surface 2 (5.7 mA/cm²) was therefore selected and kept constant in order to optimize the thickness of the porous layer. pSi with thicknesses from 1 to 4 µm were compared. An EOT decrease of 0.06%, 0.07%, 0.13%, 0.07% and 0.06% was observed for surfaces with a thickness of 1 μ m (surface 5), 1.5 μ m (surface 6), 2 μ m (surface 2), 3 μ m (surface 7) and 4 μ m (surface 8), respectively (Figure 5). Based on these results, the optimum condition for switching was obtained from the pSi with the pore size of 18 - 29 nm and the thickness of 2 μ m. For thinner layers (less than 2 μ m), the fidelity of the fringe pattern was reduced, which may have negatively impacted the magnitude of the ΔEOT . For the thicker layers (more than 2 μ m), the EOT change was similar to that for the layers with 1 μ m and 1.5 μ m thickness, which may be due to less effective polymer immobilization within the thicker layers. The optimum fabrication condition, etched at current density 5.7 mA/cm² for 810 s (Supporting information, Figure S1 for SEM images for this surface), was then used to detect different concentrations of glucose in a buffer solution at physiological pH and to determine the sensitivity of the pSi-PVPBA sensing platform.

pSiRF-PVPBA as a sensing platform for glucose

Following the success in utilizing the single layer pSi-PVPBA as an optical sensing platform for glucose detection, a pSi-based rugate filter (pSiRF) was also investigated as the sensing platform. The pSiRF was also modified and grafted with the PVPBA (pSiRF-PVPBA) in a similar fashion as for the single layer. The pSiRF structure is often found to be a more sensitive sensing platform than the single layer pSi, since a small change in the refractive index can trigger a large shift in the photonic peak of the pSiRF. 29, 41-43, 68

Fifteen periods of sinusoidal variation between the current densities of 5.7 mA/cm² and 28.3 mA/cm² for the low and high porosity layers, respectively (refer to Table 1), were applied to fabricate the pSiRF structure with a total thickness of 2.5 μ m. The pSiRF etched under these conditions displayed a characteristic photonic peak at 653.6 nm (Supporting information, Figure S3). The current density was selected from the two different pore sizes resulting in the two highest responses when the single layer pSi-PVPBA was exposed to glucose, as seen in Figure 5. The pore depth of the pSiRF was designed to have similar thickness to the optimum condition for the single layer pSi. The surface modification for the pSiRF proceeded as for single layer pSi except for the oxidation process. The freshly etched pSiRF was only oxidized using ozone for 2 h. Thermally oxidizing the thin layer of pSiRF at 600 °C damaged the photonic structure of the pSiRF, judging from the disappearance of the photonic peak after thermal oxidation.

ARTICLE

The surface modification of the pSiRF was confirmed using infrared spectroscopy. Surface modification could also be observed by monitoring the shift of photonic peak by means of IRS, since each surface modification step changes the refractive index of the porous layer and shifts the position of the photonic peak (Supporting information, Figure S3). After 2 h of ozone oxidation, a 5.8 nm blue shift was observed as the oxidation converted the surface silicon into silica that has a lower refractive index. Further modification with APTES silane, SMPB cross-linker and PVPBA-SH resulted in red shifts of 21.0 nm, 6.7 nm and 13.9 nm, respectively due to the increase of the refractive index of porous layer from the deposition of a carbonaceous layer. The observed shifts confirm the immobilization of the PVPBA on the pSiRF matrix. This sensing platform was then tested in terms of its ability to detect 10 mM of glucose in buffer solution at pH 7.4 (Figure 6).

Figure 6 presents the sensorgram obtained by IRS for the pSiRF-PVPBA. The optical detection for the pSiRF structure was performed by monitoring the shift of the photonic peak due to the change of the refractive index inside the porous layer over time. Over the first 10 min, the pSi-PVPBA was exposed to buffer solution at pH 7.4. A blue shift (shift towards shorter wavelength) was observed when the pSiRF-PVPBA surface was exposed to buffer containing 10 mM of glucose (min 11-20) and a red shift (shift towards longer wavelength) when the surface was exposed again to the buffer solution at pH 7.4. These phenomena are akin to the observed EOT changes for the single layer pSi-PVPBA. The decrease and increase in the refractive index, observed as blue and red shifts, corresponded to the reversible formation and deformation of the boronate ester, respectively.

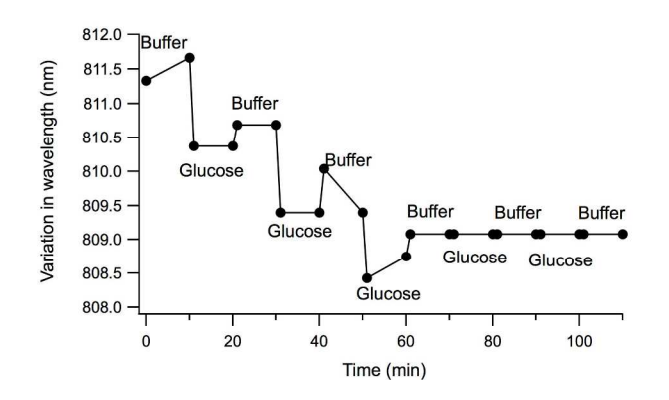


Figure 6. Variation in the photonic peak position of pSiRF-PVPBA over time when the surface was exposed to buffer solution at pH 7.4 and a buffer solution at pH 7.4 containing 10 mM glucose.

As seen in Figure 6, the immobilized PVPBA did not completely revert back to the original peak position after removal of the glucose component in buffer. For three cycles, the peak position continued to blue shift upon addition of glucose, but after removal of the glucose by washing with buffer, the sensor did not reach the position of the previous washing cycle. After 60 min (from cycle 4 onwards), there

was no reversible switching observed. This result could be interpreted in terms of glucose remaining bound to the polymer layer even during the washing step. In addition, degradation of the pSiRF-PVPBA would also be consistent with the observed results, which might be expected given the surface was only ozone treated and not thermally oxidized. Again, thermal oxidation could not be applied due to loss of the photonic peak. Considering these results, it can be concluded that the sensing platform based on single layer pSi outperformed the pSiRF. Therefore, further glucose sensing experiments focused only on single layer pSi-PVPBA.

Sensitivity of the single layer pSi-PVPBA to glucose

The sensing performance of the pSi-PVPBA platform to detect various concentrations of glucose in buffer solution at pH 7.4, ranging from 2.5 mM - 20 mM, a common range of glucose concentrations for glucose sensors based on the boronic acid polymer. 21 The ΔEOT for each concentration of glucose is presented in Figure 7.

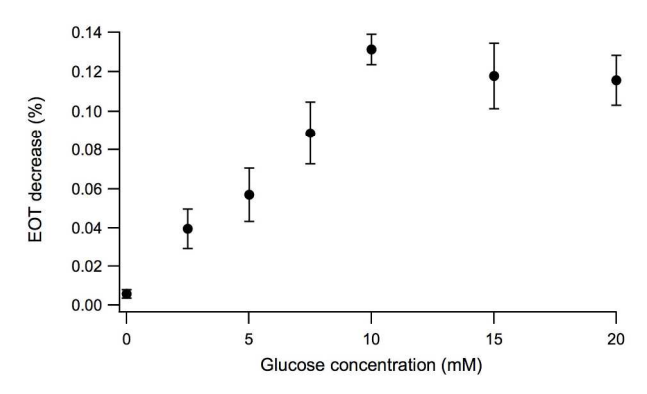


Figure 7. EOT decrease for different concentrations of glucose detected on the pSi-PVPBA film at pH 7.4. For each sample, the EOT change was taken as an average of 5 cycles of reversible switching and the error bars were calculated from 3 separate experiments.

The ΔEOT increased linearly with increasing glucose concentration from 0 mM to 10 mM ($R^2 = 0.98233$) with a sensitivity of 0.012 intensity/mM. Above this concentration, the ΔEOT slightly decreased and then plateaued, indicating that all of the boronic acid groups had been saturated with glucose. A limit of detection (LOD) was calculated using the equation of LOD = $y_b + 3Std_b$, where y_b is the value of a blank and Std_b is the standard deviation of the blank. The blank, in this case, is the pSi-PVPBA surface exposed to buffer solution that did not contain any glucose. The calculated LOD is 0.15 mM which is lower than the LOD of commercial glucose meters (0.6 mM). ⁶⁹ Therefore, by combining the properties of PVPBA with those of pSi, a glucose sensor with a linear response across the normal range of glucose levels in blood (6.1 mM \pm 1.4 mM¹), was successfully demonstrated.

Glucose detection in a human wound fluid sample

The performance of the pSi-PVPBA sensing platform has so far been investigated to detect changes in pH and glucose levels in a buffer solution. Following this, a final study looking at the responsiveness of the pSi-PVPBA to a much more complex sample, human wound fluid, was conducted. As mentioned before, the glucose level in a diabetic wound is considered indicative of the healing status of the wound.⁷

The experiments for testing the human wound fluid sample were performed in a similar way to those measuring glucose in a buffer solution. The human wound fluid sample used in this study was chronic wound fluid collected from The Queen Elizabeth Hospital (South Australia, Australia). The pH of the wound fluid sample was 8.3, as measured using a pH meter, and the glucose concentration was undetectable as measured using a commercial glucose meter (Accu Chek, Roche) (Supporting information, Figure S4(a)). The "LO" indicates a concentration of the sample lower than the working range of the glucose meter, which is 0.6 - 33.3 mM.⁶⁹ This was not surprising because the wound fluid sample was not from a diabetic wound. During sensing, the pSi-PVPBA surface was exposed to buffer solution at pH 7.4 for 10 min and then a 10-fold dilution of the wound fluid sample in Hepes buffer was exposed to the surface. The pH of the diluted wound fluid sample was 8.1. The surface was exposed to buffer/wound fluid for 5 cycles and the average ΔΕΟΤ determined. Wound fluid spiked with 10 mM of glucose was also tested (Figure 8(a)).

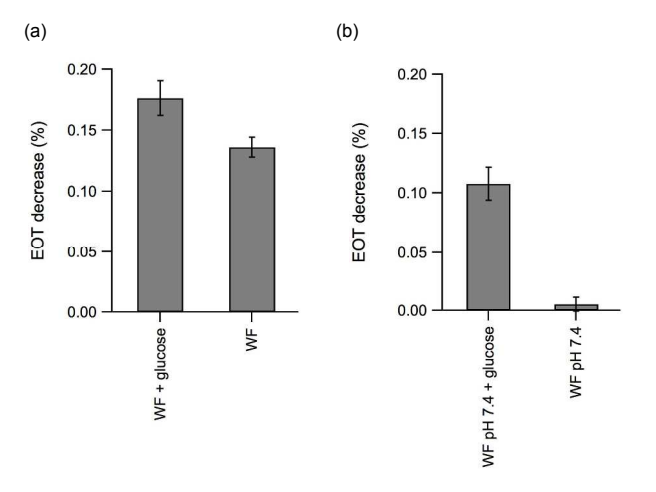


Figure 8. (a) Measured EOT decreases for pSi-PVPBA exposed to wound fluid sample (WF) and the wound fluid sample spiked with 10 mM glucose (WF + glucose). (b) Measured EOT decreases for pSi-PVPBA exposed to wound fluid sample adjusted to pH 7.4 (WF pH 7.4) and the wound fluid sample adjusted to pH 7.4 spiked with 10 mM glucose (WF pH 7.4 + glucose). For each sample, the EOT decrease was averaged from 5 cycles of reversible switching and the error bars were calculated from 3 and 8 separate experiments for Figure (a) and (b), respectively.

Exposing the pSi-PVPBA to the wound fluid significantly decreased the EOT, with the EOT changing by 0.14%. This particular wound fluid sample gave a low concentration glucose (< 0.6 mM) as indicated as "LO" on the commercial glucose meter. The shift was attributed to the slightly basic pH of the wound fluid, at which a shift in the ionization equilibrium of PVPBA occurred. When the pSi-PVPBA was exposed to the wound fluid sample that spiked with 10 mM glucose, a more pronounced decrease in EOT was observed (Δ EOT was 0.18%), showing that a further shift in the ionization equilibrium, translating into further refractive index changes was possible. However, these results suggest that the pH of the wound fluid should be adjusted before testing in order to remove the effect of pH on the Δ EOT.

The wound fluid pH (10-fold dilution) was therefore adjusted to physiological pH (pH 7.4) and then the sensing was performed as previously described, for spiked and non-spiked wound fluid (Figure 8(b)) and repeated for seven times to obtain further analytical figures

of merit. The results show that the wound fluid sample spiked with glucose decreased the EOT by 0.11% and the unspiked sample showed only a 0.01% EOT change, suggesting the change in the optical properties of the sensor in the presence of spiked wound fluid was due to the formation of anionic boronate esters with the glucose. In addition, the control experiment done using the pSi-PDMA surface (Supporting information, Figure S5) showed only a small EOT change (0.02%), corroborating the importance of boronic acid moieties in glucose detection. The small change in EOT in the unspiked wound fluid sample was in agreement with the low (LO) concentration glucose reported by the commercial glucose meter for the wound fluid sample (Supporting information, Figure S4(a)).

The 0.11% average of ΔΕΟΤ was corresponded to 8.74 mM glucose if calculated using the linear regression from Figure 7, which was done at physiological pH. The analytical figures of merit precision and accuracy were also determined. The precision corresponding to the reproducibility of measurements was 0.77 mM. The accuracy, in this case, was presented as relative percent error when it was compared to the true concentration of glucose added to the wound fluid sample since the wound fluid itself contains a low concentration of glucose (LO) as mentioned before. From the calculation, the measured concentration gave the relative percent error of 13%. For the same 10 fold dilution wound fluid sample, the commercial glucose meter gave a reading of 6.5 mM (Supporting information, Figure S4(b)) with the calculated relative percent error of 35%. These results confirm that the pSi-PVPBA sensor gave a closer reading to the actual glucose concentration in the sample than the commercial glucose meter (which is optimized for blood). Wound fluid is a complex matrix that contains a large range of proteins and enzymes but did not noticeably affect the sensing performance of the pSi-PVPBA sensor.

Conclusions

We demonstrated an optical biosensor based on a pSi thin film with grafted PVPBA as a pH- and glucose-responsive polymer. The phenylboronic acid of the PVPBA exists in the equilibrium between a neutral trigonal form and an anionic tetrahedral form, with the equilibrium driven by the pH of solution or the presence of glucose. The surface modification steps and the immobilization of the polymer were confirmed by DRIFT-IR. The behavior of the immobilized polymer in response to the pH changes and the presence of glucose at physiological pH were studied optically by means of IRS. The reversible formation of neutral and anionic forms of the PVPBA was observed as a reversible increase and decrease in the EOT of the pSi-PVPBA film, respectively.

The application of the pSi-PVPBA as a sensing platform was also demonstrated. Pore size and pore thickness of single layer pSi-PVPBA films were optimized and a photonic pSi rugate filter was also tested. The optimum conditions for a single layer pSi film were then used to detect various glucose concentrations, ranging from 0 mM to 20 mM with a calculated limit of detection of 0.15 mM. Finally, sensing experiments using a human wound fluid sample were performed, which show that the pSi-PVPBA was sensitive to the pH of the wound fluid sample, which was slightly basic. By adjusting the pH of wound fluid sample to physiological pH, the sensor was able to selectively detect glucose spiked into the wound fluid with low levels of interference, outperforming a commercial glucose meter. With further development, this sensing platform may find practical applications in chronic wound prognostics, as glucose levels in chronic wounds are indicative of the healing trajectory.

13

15

16

Acknowledgements

ARTICLE

The authors would like to thank Allison Cowin and Elizabeth Melville from the Mawson Institute for providing human wound fluid samples, Roshan Vasani for important discussions on the experimental setup and results interpretation, the Wound Management Innovation CRC for funding, and the University of South Australia for a PhD scholarship for FSHK. WLAB and BSS acknowledge the National Science Foundation (DMR-0846792) for partial support of this work.

Notes and references

- ^a Mawson Institute, University of South Australia, Adelaide, South Australia 5095 Australia
- ^b George & Josephine Butler Polymer Research Laboratory, Center for Macromolecular Science & Engineering, Department of Chemistry, University of Florida, PO Box 117200, Gainesville, FL 32611-7200, USA
- * Corresponding authors:

Prof. Nicolas H. Voelcker

Email: nico.voelcker@unisa.edu.au

Tel: +61 8 8302 5508; Fax: +61 8 8302 5613

Prof. Brent S. Sumerlin

Email: sumerlin@chem.ufl.edu

Tel: (352) 392-0563

Electronic Supplementary Information (ESI) available: [details of any supplementary information available should be included here]. See DOI: 10.1039/b000000x/

- E. Wilkins and P. Atanasov, *Medical Engineering Physics*, 1996, **18**, 273-288.
- 2 WHO, Diabetes Mellitus, http://www.who.int/mediacentre/factsheets/fs138/en/, Accessed 23 October, 2013.
- 3 T. J. Fahey, A. Sadaty, W. G. Jones, A. Barber, B. Smoller and G. T. Shires, *Journal of Surgical Research*, 1991, **50**, 308-313.
- W. H. Goodson and T. K. Hunt, *The Journal of Surgical Research*, 1977, **22**, 221-227.
- N. Collins and R. Toiba, *Ostomy Wound Management*, 2010, **September 2010**, 18-24.
- C. Wetzler, H. Kampfer, B. Stallmeyer, J. Pfeilschifter and S. Frank, *J. Invest. Dermatol.*, 2000, 115, 245-253.
- 7 P. Velander, C. Theopold, T. Hirsch, O. Bleiziffer, B. Zuhaili, M. Fossum, D. Hoeller, R. Gheerardyn, M. Chen, S. Visovatti, H. Svensson, F. Yao and E. Eriksson, *Wound Rep. Reg.*, 2008, **16**, 288-293.
- 8 E.-H. Yoo and S.-Y. Lee, *Sensors*, 2010, **10**, 4558-4576.
- 9 J. Wang, Chemical Reviews, 2008, **108**, 814-825.
- J. Hönes, P. Müller and N. Surridge, *Diabetes Technology & Therapeutics*, 2008, 10, S10-S26.
- D. Roy, J. N. Cambre and B. S. Sumerlin, *Progress in Polymer Science*, 2010, **35**, 278-301.
- S. Kitano, Y. Koyama, K. Kataoka, T. Okano and Y. Sakurai, *J. Controlled Release*, 1992, **19**, 162-170.

- Z. Gu, T. T. Dang, M. Ma, B. C. Tang, H. Cheng, S. Jiang, Y. Dong, Y. Zhang and D. G. Anderson, *ACS NANO*, 2013, 7, 6758-6766.
- Z. Gu, A. A. Aimetti, Q. Wang, T. T. Dang, Y. Zhang, O. Veiseh, H. Cheng, R. S. Langer and D. G. Anderson, ACS NANO, 2013, 7, 4194-4201.
 - K. Kataoka, H. Miyazaki, M. Bunya, T. Okano and Y. Sakurai, *J. Am. Chem. Soc.*, 1998, **120**, 12694-12695.
 - D. Shiino, K. Kataoka, Y. Koyama, M. Yokoyama, T. Okano and Y. Sakurai, *Journal of Intelligent Material Systems and Structures*, 1994, **5**, 311-314.
- D. Roy, J. N. Cambre and B. S. Sumerlin, *Chem. Commun.*, 2009.
- D. Roy and B. S. Sumerlin, American Chemical Society Macro Letters, 2012, 1, 529-532.
- M. B. Lerner, N. Kybert, R. Mendoza, R. Villechenon, M. A. B. Lopez and A. T. C. Johnson, *Appl. Phys. Lett.*, 2013.
- D. Roy, J. N. Cambre and B. S. Sumerlin, *Chem. Commun.*, 2008, 2477-2479.
- J. N. Cambre, D. Roy and B. S. Sumerlin, Journal of Polymer Science Part A: Polymer Chemistry, 2012, 50, 3373-3382
- A. Stephenson-Brown, H.-C. Wang, P. Iqbal, J. A. Preece, Y. Long, J. S. Fossey, T. D. James and P. M. Mendes, *Analyst*, 2013.
- A. Kikuchi, K. Suzuki, O. Okabayashi, H. Hoshino, K. Kataoka, Y. Sakurai and T. Okano, *Anal. Chem.*, 1996, 68, 823-828.
- V. L. Alexeev, A. C. Sharma, A. V. Goponenko, S. Das, I. K. Lednev, C. S. Wilcox, D. N. Finegold and S. A. Asher, *Anal. Chem.*, 2003, 75, 2316-2323.
- S. Tierney, S. Volden and B. T. Stokke, *Biosens. Bioelectron.*, 2009, 24, 2034-2039.
- O. B. Ayyub, J. W. Sekowski, T.-I. Yang, X. Zhang, R. M. Briber and P. Kofinas, *Biosens. Bioelectron.*, 2011, 28, 349-354.
- A. Jane, R. Dronov, A. Hodges and N. H. Voelcker, *Trends Biotechnol.*, 2009, **27**, 230-239.
- C. Pacholski, M. Sartor, M. J. Sailor, F. Cunin and G. M. Miskelly, *J. Am. Chem. Soc.*, 2005, 127, 11636-11645.
- 29 T. Bocking, K. A. Kilian, K. Gaus and J. J. Gooding, *Adv. Funct. Mater.*, 2008, **18**, 3827-3833.
- L. A. DeLouise, P. M. Fauchet, B. L. Miller and A. A. Pentland, *Adv. Mater.*, 2005, 17, 2199-2203.
- V. S.-Y. Lin, K. Motesharei, K. Dancil, M. J. Sailor and M. R. Ghadiri, *Science*, 1997, 278, 840-843.
- B. Gupta, Y. Zhu, B. Guan, P. J. Reece and J. J. Gooding, *Analyst*, 2013, 138, 3593-3615.
- 33 E. J. Anglin, L. Cheng, W. R. Freeman and M. J. Sailor, Adv. Drug Delivery Rev., 2008, 60, 1266-1277.
 - F. S. H. Krismastuti, A. J. Cowin, S. Pace, E. Melville, T. R. Dargaville and N. H. Voelcker, *Aust. J. Chem.*, 2013, **66**, 1428-1434.
- S. Pace, R. B. Vasani, F. Cunin and N. H. Voelcker, *New J. Chem.*, 2013, 37, 228-235.
- 36 R. B. Vasani, S. J. P. McInnes, M. A. Cole, A. M. M. Jani, A. V. Ellis and N. H. Voelcker, *Langmuir*, 2011, 27, 7843-7853.
- S. P. Low, N. H. Voelcker, L. T. Canham and K. A. Williams, *Biomaterials*, 2009, 30, 2873-2880.
- N. H. Voelcker, I. Alfonso and M. R. Ghadiri, ChemBioChem, 2008, 8, 1776-1786.
- 39 K.-P. S. Dancil, D. P. Greiner and M. J. Sailor, *J. Am. Chem. Soc.*, 1999, **121**, 7925-7930.

67

68

Journal Name

- 40 E. Lorenzo, C. J. Oton, N. E. Capuji, M. Ghulinyan, D. Navarro-Urrios, Z. Gaburro and L. Pavesi, *Applied Optics*, 2005, **44**, 5415-5421.
- 41 K. A. Kilian, T. Bocking, S. Ilyas, K. Gaus, W. Jessup, M. Gal and J. J. Gooding, *Adv. Funct. Mater.*, 2007, 17, 2884-2890
- 42 K. A. Kilian, T. Bocking and J. J. Gooding, *Chem. Commun.*, 2009, 630-640.
- 43 K. A. Kilian, K. Gaus, M. Gal and J. J. Gooding, ACS NANO, 2007, 1, 355-361.
- 44 L. De Stefano, E. De Tommasi, I. Rea, L. Rotiroti, M. Canciello, G. Maglio and R. Palumbo, *Applied Physics A*, 2010, **98**, 525-530.
- 45 L. De Stefano, L. Rotiroti, E. De Tommasi, I. Rea, I. Rendina, M. Canciello, G. Maglio and R. Palumbo, *J. Appl. Phys.*, 2009, **106**, 0023109-0023101-0023105.
- 46 N. A. Tokranova, S. W. Novak, J. Castracane and I. A. Levitsky, *The Journal of Physical Chemistry C*, 2013, **117**, 22667-22676.
- 47 J. Wu and M. J. Sailor, Adv. Funct. Mater., 2009, 19, 733-741.
- 48 E. Segal, L. A. Perelman, F. Cunin, F. Di Renzo, J. M. Devoisselle, Y. Y. Li and M. J. Sailor, *Adv. Funct. Mater.*, 2007, **17**, 1153-1162.
- J. T. Lai, D. Filla and R. Shea, *Macromolecules*, 2002, 35, 6754-6756.
- J. N. Cambre, D. Roy, S. Gondi and B. S. Sumerlin, *J. Am. Chem. Soc.*, 2007, 129, 10348-10349.
- S. Pace, B. Seantier, E. Belamie, N. Lautrédou, M. J. Sailor, P.-E. Milhiet and F. Cunin, *Langmuir*, 2012, 28, 6960-6969.
- 52 H. Ouyang, M. Christophersen, R. Viard, B. L. Miller and P. M. Fauchet, Adv. Funct. Mater., 2005, 15, 1851-1859.
- B. Sciacca, E. Secret, S. Pace, P. Gonzalez, F. Geobaldo, F. Quignard and F. Cunin, *J. Mater. Chem.*, 2011, 21, 2294.
- J. Salonen and V.-P. Lehto, *Chemical Engineering Journal*, 2008, **137**, 162-172.
- D. B. Mawhinney, J. A. Glass and J. T. Yates, *J. Phys. Chem. B*, 1997, **101**, 1202-1206.
- A. Janshoff, K.-P. S. Dancil, C. Steinem, D. P. Greiner, V. S.-Y. Lin, C. Gurtner, K. Motesharei, M. J. Sailor and M. R. Ghadiri, J. Am. Chem. Soc., 1998, 120, 12108-12116.
- 57 M. J. Sweetman, C. J. Shearer, J. G. Shapter and N. H. Voelcker, *Langmuir*, 2011, **27**, 9497-9503.
- 58 E. T. Vandenberg, L. Bertilsson, B. Liedberg, K. Uvdal, R. Erlandsson, H. Elwing and I. Lundstrom, *Journal of Colloid and Interface Science*, 1991, 147.
- N. Aissaoui, L. Bergaoui, J. Landoulsi, J.-F. Lambert and S. Boujday, *Langmuir*, 2012, 28, 656-665.
- B. Xia, S.-J. Xiao, D.-J. Guo, J. Wang, J. Chao, H.-B. Liu,
 J. Pei, Y.-Q. Chen, Y.-C. Tang and J.-N. Liu, *J. Mater. Chem.*, 2006, 16, 570-578.
- 61 H. Chen, M. Lee, J. Lee, J.-H. kim, Y.-S. Gal, Y.-H. Hwang, W. G. An and K. Koh, *Sensors*, 2007, 7.
- 62 J. A. Faniran and H. F. Shurvell, Canadian Journal of Chemistry, 1968, 46, 2089-2095.
- J. N. Cambre and B. S. Sumerlin, *Polymer*, 2011, 52, 4631-4643.
- 64 K. T. Kim, J. J. L. M. Cornelissen, R. J. M. Nolte and J. C. M. van Hest, J. Am. Chem. Soc., 2009, 131, 13908-13909.
- 65 R. Ma, H. Yang, Z. Li, G. Liu, X. Sun, X. Liu, Y. An and L. Shi, *Biomacromolecules*, 2012, **13**, 3409-3417.

- C. Zhang, M. D. Losego and P. V. Braun, *Chemistry of Materials*, 2013, **25**, 3239-3250.
- B. Pappin, M. J. Kiefel and T. A. Houston, in *Carbohydrates Comprehensive Studies on Glycobiology* and *Glycotechnology*, Intech, 2012.
 - B. Guan, A. Magenau, K. A. Kilian, S. Ciampi, K. Gaus, P. J. Reece and J. J. Gooding, *Faraday Discuss.*, 2011, **149**, 301-317.
 - J. Kozar, A.-M. Šimundić, N. Nicolac, M. Žirović and E. Topić, *Biochemia Medica*, 2008, **18**, 361-367.

Graphical abstract

A Photonic Glucose Biosensor for Chronic Wound Prognostics

Fransiska S. H. Krismastuti, William L. A. Brooks, Martin J. Sweetman, Brent S. Sumerlin, Nicolas H. Voelcker^a,*

^aMawson Institute, University of South Australia, Adelaide, South Australia 5095, Australia

^bGeorge & Josephine Butler Polymer Research Laboratory, Center for Macromolecular Science & Engineering, Department of Chemistry, University of Florida, PO Box 117200, Gainesville, FL 32611-7200, USA

*Corresponding authors:

Prof. Nicolas Voelcker

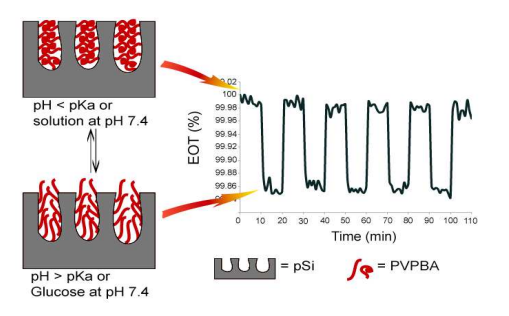
Email: nico.voelcker@unisa.edu.au

Tel: +61 8 8302 5508; Fax: +61 8 8302 5613

Prof. Brent S. Sumerlin

Email: sumerlin@chem.ufl.edu

Tel: (352) 392-0563



An optical biosensor based on the switching of Poly(4-vinylphenylboronic acid) (PVPBA) grafted to the pores of porous silicon (pSi) films in response to pH and glucose.